

LMU

LUDWIG-
MAXIMILIANS-
UNIVERSITÄT
MÜNCHEN

CENTER FOR QUANTITATIVE RISK ANALYSIS
CEQURA



Andreas Fuest and Stefan Mittnik

Modeling Liquidity Impact on Volatility: A GARCH-FunXL Approach

Working Paper Number 15, 2015
Center for Quantitative Risk Analysis (CEQURA)
Department of Statistics
University of Munich

<http://www.cequra.uni-muenchen.de>



Modeling Liquidity Impact on Volatility: A GARCH-FunXL Approach

Andreas Fuest* & Stefan Mittnik*

First version: January 19, 2015

This version: July 13, 2015

Abstract

We introduce a new semiparametric model, GARCH with *Functional* EXogeneous Liquidity (GARCH-FunXL), to capture the impact of liquidity, as implied by a stock exchange's complete electronic limit order book (LOB), on asset price volatility. LOB-implied liquidity can be viewed as a *functional* rather than scalar or vectorial stochastic process. We adopt recent ideas from the functional data analysis (FDA) literature to link scalar conditional return volatility to curve-valued liquidity.

Simulation experiments for a log-GARCH version of the model show that it works well in finite samples. Applying our new methodology to intraday return data from the German XETRA system, we find a substantial liquidity impact on return variation. Finally, we show that the forecast performance of the GARCH-FunXL model is clearly superior as compared to a model without liquidity impact.

JEL classification: C22, C55, C58, G14

Keywords: limit order book, functional data, GARCH-X, liquidity, high-frequency data

**Address for correspondence:* Chair of Financial Econometrics, Center for Quantitative Risk Analysis, Ludwig-Maximilians-Universität München, Akademiestrasse 1/I, 80799 Munich, Germany; Phone: +49 (0)89 2180-3522; Email: {fuest, finmetrics}@stat.uni-muenchen.de. Comments and suggestions are appreciated. We thank Robert Engle, Matthias Fengler, Timo Teräsvirta, participants of the 8th Annual SoFiE Conference 2015 in Aarhus, and participants of the Workshop on Non- and Semiparametric Volatility and Correlation Models 2014 in Paderborn for valuable discussions and suggestions.

1 Introduction

The recent availability of high-frequency financial data has helped to deepen our understanding of the microstructure of financial markets. At the same time, the microstructure itself has changed as electronic order-driven trading platforms have become, de facto, the standard for trading of financial securities. In the econometric literature on high-frequency data, starting in the 1990s, two major strands have developed. The first is concerned with the dynamic properties of the trading process as a whole, i.e., not only of prices but also of trading volume, bid-ask spreads etc., as well as their interactions. Financial duration models pioneered by [Engle and Russell \(1998\)](#) and [Engle \(2000\)](#) and their various applications are the most prominent examples of this line of research. The second strand can be termed *realized volatility*. It aims at using high-frequency information on *prices* to improve the measurement of price volatility and, in a second step, modeling volatility dynamics. In other words, the realized volatility project has the same goals as, say, GARCH modeling daily data, but hopes to improve accuracy by looking at higher sampling frequencies.

The present paper contributes to the literature by bringing together a traditional dynamic GARCH volatility model with the complete (in a cross-sectional sense) "micro-state of the market" for a financial security as implied by its limit order book (LOB).

To sketch the idea, consider a linear GARCH(1,1) specification for intraday, de-seasonalized log-returns, $r_{t,i} = \log P_{t,i} - \log P_{t,i-1}$, on the mid-quote, $P_{t,i}$, at intraday time i and trading day t ,

$$r_{t,i} = \sigma_{t,i} \varepsilon_{t,i}, \quad \varepsilon_{t,i} \stackrel{iid}{\sim} (0, 1), \quad \sigma_{t,i}^2 = \omega + \alpha r_{t,i-1}^2 + \beta \sigma_{t,i-1}^2, \quad (1)$$

as it has been applied, for instance, by [Engle and Sokalska \(2012\)](#) to 10-minute returns on the New York Stock Exchange (NYSE). The LOB however does not only reveal information on prices, but also on the size of limit orders around the quotes, the LOB inventories. Figure 1 illustrates the state of a LOB at some given time during a trading day. We denote the left curve, the bid curve, by $x_{t,i}^{(bid)}(P)$ and the right curve, the ask curve, by $x_{t,i}^{(ask)}(P)$, and view them as functions of the price.

Now consider the case where order book inventories, $x_t^{(ask)}(P)$ say, have an impact on the price. We extend the model introduced above by capturing possible effects of these function-valued objects on the variation of the price by specifying the conditional variance in terms of

$$\sigma_{t,i}^2 = \omega + \alpha r_{t,i-1}^2 + \beta \sigma_{t,i-1}^2 + \int_{\mathcal{P}} \gamma(m) x_{t,i-1}^{(ask)}(m) dm, \quad (2)$$

where \mathcal{P} is the interval of possible prices. Extension (2) is now of the GARCH-X type but, in contrast to existing specifications of this kind, the exogenous variable is a curve-valued, i.e., infinite-dimensional quantity. In fact, $\int_{\mathcal{P}} \gamma(m) x_{t,i-1}^{(ask)}(m) dm$

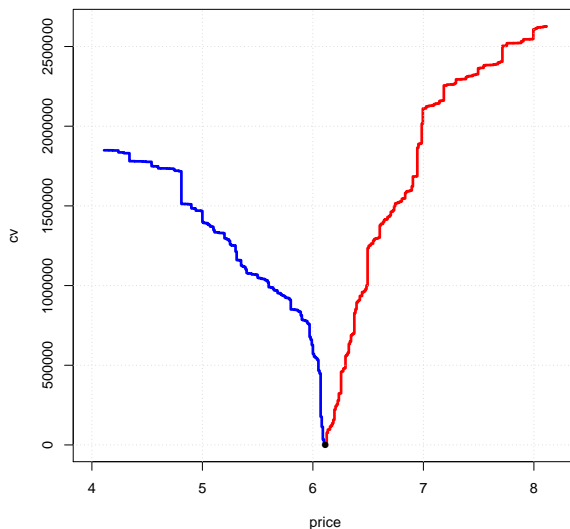


Figure 1: *State of a limit order book at some time during the trading day, consisting of (i) prices, i.e. bid and ask quotes whose mean (the mid-quote) is represented by a dot, and (ii) liquidity, represented by the available requested (left) and offered (right) cumulative number of shares as a function of the price.*

is the limit case of a linear predictor, where $\gamma(m)$ is a functional rather than a vectorial parameter, mapping liquidity at all price levels $P \in \mathcal{P}$ to scalar conditional volatility.

Early studies on the connection of liquidity and volatility (e.g., Gallant et al. (1992), Jones et al. (1994)) employ daily transactions data to measure liquidity. More recently, the structure (Gouriéroux et al., 1998) and dynamics (Härdle et al. (2012); Bowsher (2004) in an early version of Bowsher and Meeks (2008)) of liquidity as implied by an order-driven market have been studied. The GARCH-FunXL approach proposed here is, to the best of our knowledge, the first attempt to model volatility dynamics using the full LOB.

The remainder of the paper is organized as follows: Section 2 explains in detail how liquidity curves, sampled intradaily at a constant frequency, are constructed from LOB data and parsimoniously represented in the framework of functional time series analysis. Basic empirical properties of these curves are evaluated for three liquid stocks traded on the German XETRA system. Section 3 introduces the GARCH-FunXL model. A two-step QML estimation procedure for the model's parameters, especially the functional parameter $\gamma(m)$, is developed and the different sources of estimation uncertainty are discussed. In a simulation study we investigate the finite-sample performance of the estimation strategy. In an empirical application presented in Section 4, the model is fitted to the three XETRA stocks. Both in-sample results and out-of-sample forecast evaluations underline the relevance of liquidity for explaining price variation. Section 5 concludes the paper.

2 Liquidity

Limit order books carry dynamic information on price and liquidity of an asset. Strictly speaking, the price is an implication of the state of liquidity. Nevertheless, as will be detailed next, it is possible to measure both phenomena separately.

2.1 Limit order book information

Regardless of the specific market design (limit order book or competing market makers), information on the current price and liquidity of a stock is given by the requested (demand) and offered (supply) volume of shares around the quotes. The latter are an implication of the offers and requests: The bid quote is the highest supply price, the ask quote is the lowest demand price. The difference of the two is always at least one tick.

LOB_t , the state of the limit order book at some time t during a trading day, can be characterized by $P_t^{(s)}$, $s \in \{bid, ask\}$, the quotes (measured in ticks), and $v_t^{(s)}(d)$, the outstanding number of shares on market side s and at a price distance of d ticks from the respective quote. In the following, we call d the *relative price* or *distance*. As limit sell orders may, in principle, be posted at any integer number, we write $d_t^{max} = \max\{d | v_t^{(ask)}(d) > 0\}$ for supply at the highest relevant price to characterize the *dimension* of LOB_t . Limit buy orders can be posted at any price level between (but excluding) zero and the ask quote.

Then, the LOB at time t is given by the $D_t = (P_t^{(bid)} + d_t^{max} + 3)$ -dimensional vector

$$LOB_t := [P_t^{(bid)}, P_t^{(ask)}, v_t^{(bid)}(P_t^{(bid)} + 1), \dots, v_t^{(bid)}(0), v_t^{(ask)}(0), \dots, v_t^{(ask)}(d_t^{max})]'$$

D_t is typically very large, and the pattern of active orders (i.e., all tuples {price, # shares, market side}) highly irregular.

Adding up the demand (supply) in the market at a given relative price, we obtain the cumulative volume.

Definition 1 (Cumulative volume, cumulative imbalance). *Let $v_t^{(s)}(d)$, $d = 0, 1, 2, \dots$ be the volume in the book at a distance of d ticks from the best quote on market side $s \in \{bid, ask\}$. The cumulative volume (CV) at side s , tick d and time t is defined by*

$$x_t^{(s)}(d) = \sum_{k=0}^d v_t^{(s)}(k),$$

and the cumulative imbalance at tick d and time t by

$$x_t^{(imb)}(d) = x_t^{(ask)}(d) - x_t^{(bid)}(d).$$

There is a one-to-one relationship between CV and the average price per share as a function of the offered/requested market order volume as has been analyzed in Gouriéroux et al. (1998) and Bowsher (2004). If the volumes in the book are weighted by their prices, the resulting quantity is called *depth*. Therefore, the depth of an order book is a hybrid between a liquidity measure and a measure of the price of an asset. As we seek to analyze liquidity impact on the price process, we will use CV as our liquidity measure. A possible drawback of this approach is that a comparison of the liquidities of different stocks becomes more complicated.

In the following, we call the mid-quote, $P_t := (P_t^{(bid)} + P_t^{(ask)})/2$, the *price* of the asset. Assuming an equidistant sampling scheme at frequency $1/\Delta$, the log-return of the price is given by $r_t = \log P_t - \log P_{t-\Delta}$. Confining ourselves to only a single constant sampling frequency, we set $\Delta := 1$ without loss of generality.

Cumulative volume curves are termed (bid or ask) *liquidity* in the remainder of the paper.

2.2 Diurnal patterns

As discussed next, the behaviour of price volatility and liquidity exhibits certain regularities during a trading day that can be treated as being deterministic. In case of volatility, this is the well-known U-shape over the trading day; for liquidity, the pattern is a bivariate function of both time-of-day and relative price.

2.2.1 Volatility pattern

As we are interested in asset returns at high frequency, we introduce a second time index or clock, so that $r_{t,i}$ denotes the i -th of I raw intraday returns on day t , $t = 1, \dots, T$. Following Andersen and Bollerslev (1997), Andersen and Bollerslev (1998) and Engle and Sokalska (2012), we assume that the raw return is given by the product of a stochastic component, $y_{t,i}$, and a deterministic diurnal component, s_i , i.e.,

$$r_{t,i} = y_{t,i}s_i.$$

Our interest centers on the conditional variance of the stochastic part, $y_{t,i}$. The deterministic diurnal pattern, s_i , can be estimated as the mean squared return at the specific intraday interval, $\hat{s}_i = T^{-1} \sum_{t=1}^T r_{t,i}^2$ (Engle and Sokalska, 2012), or a smoothed version thereof. Andersen and Bollerslev (1997), for instance, use the flexible Fourier functional form proposed by Gallant (1981), where smoothness of the fitted pattern is implicitly imposed through the choice of constant and cyclical components.

Similar to this second approach, we use a cubic smoothing spline to fit the scatterplot of squared intraday returns vs. (intraday) time, where the smoothing

parameter is chosen via generalized cross validation. Results are shown in Section 2.5.

2.2.2 Liquidity pattern

Curve-valued liquidity can be decomposed in an analogous way. Here, for each market side, the diurnal pattern is itself a deterministic function of the relative price d and intraday time i . Raw liquidity on market side s , $\tilde{x}_{t,i}^{(s)}$, is given by

$$\tilde{x}_{t,i}^{(s)}(d) = \nu_i^{(s)}(d)x_{t,i}^{(s)}(d),$$

where $\nu_i(d)$ is the deterministic diurnal liquidity surface and $x_{t,i}^{(s)}(d)$ the stochastic liquidity component, which is of primary interest in our analysis.

As the pattern is typically less pronounced than the volatility pattern, we do not smooth the diurnal pattern (which could in principle easily be done, for example by using a tensor product spline) but rather use simple averaging. The estimator is then given by

$$\hat{\nu}_i^{(s)}(d_j) = T^{-1} \sum_{t=1}^T \tilde{x}_{t,i}^{(s)}(d_j),$$

where d_1, \dots, d_J is the observation grid along the price axis. Empirical results are shown in Section 2.5.

2.3 Liquidity as functional time series

In the following, assume that relative prices, originally observed on a tick grid, are rescaled to lie in $[0, 1]$, i.e., $0 = d_1 < \dots < d_J = 1$. Dropping the superscript “(s)” for this exposition, we assume the de-seasonalized liquidity curves for each market side to be generated by a functional stochastic process in discrete time, $(x_t)_{t \in \mathbb{Z}}$, whose observations are elements of the Hilbert space $L^2([0, 1])$ with inner product $\langle x, y \rangle := \int_0^1 x(s)y(s)ds$, so that x_t is assumed to be square integrable.

The liquidity process exhibits a mean function, $\mu(d) := E[x_t(d)]$, and a (contemporaneous) covariance operator $C(z)[\langle x - \mu, z \rangle(x - \mu)]$ with covariance kernel $\Sigma(d, m) = \text{Cov}(x_t(d), x_t(m))$. Mean and covariance kernel are constant over time. The covariance operator has the form

$$C(z)(d) = \int_0^1 \Sigma(d, m)z(m)dm,$$

describing the contemporaneous linear dependence of different locations (relative prices) of a liquidity curve. The quantities μ and Σ can be viewed as the functional time series analogues to the unconditional mean vector and the lag-zero autocovariance matrix in vector autoregression. The covariance operator admits the spectral representation

$$C(z) = \sum_{j=1}^{\infty} \lambda_j \langle \phi_j, z \rangle \phi_j,$$

where the λ_j are the (strictly decreasing) eigenvalues and the ϕ_j are the corresponding orthonormal eigenfunctions of C , i.e., $\int_0^1 \phi_j^2(m) dm = 1$ and $\int_0^1 \phi_k(m) \phi_j(m) dm = 0$, $k \neq j$ hold. The $\xi_{j,t} := \langle \phi_j, x_t \rangle$ are called the scores or loadings of the j -th eigenfunction on liquidity at time t .

Based on the spectral representation, liquidity curves can then be represented via the Karhunen-Loève decomposition,

$$x_t(d) = \mu(d) + \sum_{j=1}^{\infty} \xi_{j,t} \phi_j(d),$$

which is also called the functional principal component (FPC) representation. The eigenvalues λ_j of the spectral representation are equal to the unconditional variances of the FPC scores $\xi_{j,t}$. As the eigenvalues are strictly decreasing, the FPCs are sorted by their contribution to the x_t 's (unconditional) variation. This gives rise to the K -truncated FPC representation

$$x_t(d) = \mu(d) + \sum_{j=1}^K \xi_{j,t} \phi_j(d) + v_t(d),$$

where $v_t(d) = \sum_{j=K+1}^{\infty} \xi_{j,t} \phi_j(d)$ is the truncation error.

In practice, we are interested in approximating the curves using such a truncation. The smallest number of components, K , necessary to explain a certain proportion (say 99%) of the curves' total variation is called the *effective dimension* of the liquidity process.

In many applications in functional data analysis, either the observation grid is irregular and/or sparse, or some measurement errors on the observed x_t are present. In all these cases, x_t can not directly be observed but must be estimated — usually in a nonparametric way. For our LOB data, however, none of these problems are present: The relative price grid is dense and equidistant, there are no missing values, and the measurement can be considered to be exact.

2.4 Estimation

At this point, the question arises how mean and eigenfunctions can be estimated from data, and how to obtain the empirical FPC scores $\hat{\xi}_{j,t}$. In practice, we observe discrete versions of the curves, \mathbf{x}_t , on the grid d_1, \dots, d_J , such that the realization of each curve is a J -dimensional vector. Raw estimates of mean function and covariance kernel are then given by

$$\hat{\mu}(d_j) = \frac{1}{T} \sum_{t=1}^T x_t(d_j), \quad d_j \in [0, 1],$$

and, with $\hat{\boldsymbol{\mu}} := [\hat{\mu}(0) \ \hat{\mu}(d_2) \ \cdots \ \hat{\mu}(d_{J-1}) \ \hat{\mu}(1)]'$ and $\mathbf{X}^c = [\mathbf{x}_1 - \hat{\boldsymbol{\mu}} \ \cdots \ \mathbf{x}_T - \hat{\boldsymbol{\mu}}]'$,

$$\hat{\boldsymbol{\Sigma}} = \frac{1}{T} \mathbf{X}^{c'} \mathbf{X}^c.$$

The eigenvalues and eigenfunctions of the raw covariance kernel $\hat{\boldsymbol{\Sigma}}$ can then, in practice, be computed using standard software for singular value decomposition. Given these, the empirical FPC scores $\hat{\xi}_{j,t} = \int_0^1 (x_t(m) - \hat{\mu}(m)) \hat{\phi}_j(m) dm$ can be obtained by numerical integration. An estimator for the covariance operator itself is then given by

$$\hat{C}(z) = \frac{1}{T} \sum_{t=1}^T \langle x_t - \hat{\boldsymbol{\mu}}, z \rangle (x_t - \hat{\boldsymbol{\mu}}).$$

Although the observed liquidity curves are step functions by construction, it may be convenient — especially with a view to the desired K -dimensional approximation — to interpret them as realizations of a process generating intrinsically smooth curves. There are several ways this can be achieved: by smoothing the observed x_t in the first place and then using discrete versions of these smoothed objects when estimating mean and covariance operator, or by smoothing mean and eigenfunctions after estimation.

Our strategy is to use the raw mean function, which we found to be already quite smooth in our applications. In case of the covariance kernel, we smooth the raw covariance kernel, $\hat{\boldsymbol{\Sigma}}$, using the sandwich smoother of [Xiao et al. \(2013\)](#). Alternatives would be kernel smoothing ([Staniswalis and Lee, 1998](#); [Yao et al., 2005](#)) or penalized tensor product splines ([Di et al., 2009](#)). Moreover, we found that in our applications eigenfunction estimates based on smoothed and raw covariance kernel estimates do not differ much, so that the smoothing step is not indispensable.

The estimation procedure described so far was originally designed for the case of *iid* data. Recently, [Hörmann and Kokoszka \(2010\)](#) introduced a stationarity concept for functional time series, called *L^p - m -approximability*, under which $\hat{\boldsymbol{\mu}}$ and $\hat{C}(z)$ are \sqrt{T} -consistent. Throughout, we assume our liquidity process(es) to be stationary in this sense.

2.5 Empirical results

Next, we discuss estimation of the diurnal patterns and the FPCs for the data at hand. Before doing so, we provide a description of the data.

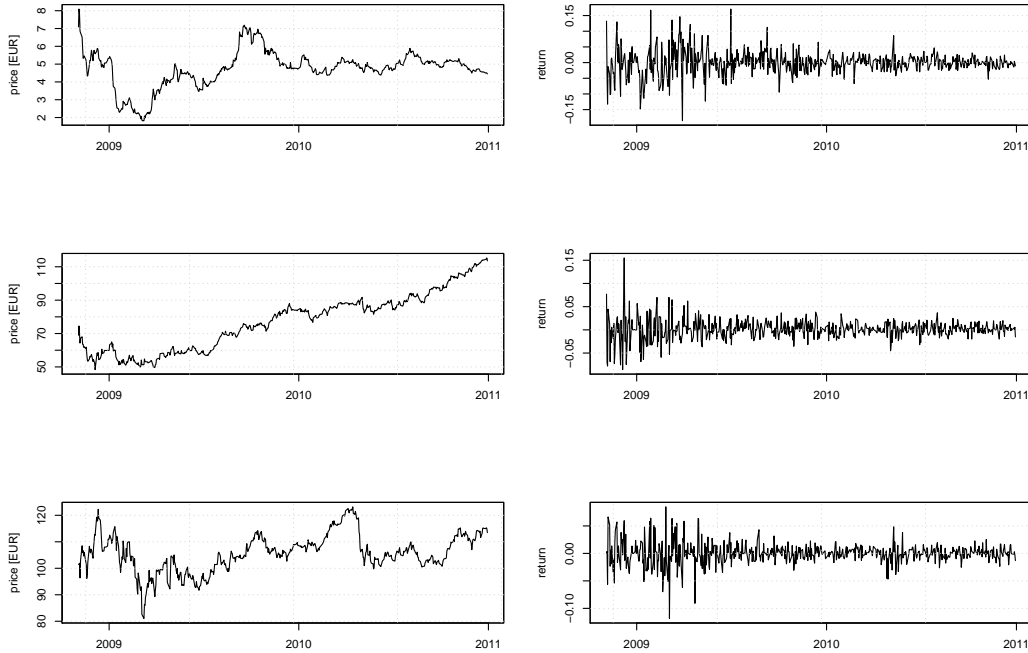


Figure 2: Daily closing prices (left panel) and log returns (right panel) for Commerzbank (upper panel), Linde (center panel), and MunichRe (bottom panel).

2.5.1 Data

We use historical limit order book data from the German XETRA system from November 3, 2008 to December 31, 2010, obtained from the Deutsche Börse AG. The data set covers 531 trading days and contains information on all limit order submissions, revisions, cancellations, and all trades (i.e., market orders) at all permissible price levels for three DAX constituents: Linde, an industrial company; Commerzbank; and the (re-)insurance company MunichRe.¹

The sample starts in midst of the global financial crisis and ends in a more tranquil period. Figure 2 gives a first impression of the “longer-run” behavior during the 26 months, showing the daily closing prices and the corresponding returns. The price levels of the three stocks behave quite differently during this period: Linde experienced a positive trend, MunichRe a sideways market, and Commerzbank stabilized in the second half after some turmoil in early 2009. In contrast, the dispersion patterns over time are quite similar for all three stocks.

The permissible price levels are given by the positive multiples of the tick size.

¹For Commerzbank (MunichRe, Linde), 530 (526, 529) full trading days have been observed, with 25 daily snapshots each, amounting to 13250 (13150, 13225) observations, from which we compute 24 intraday returns per day. After removing the diurnal volatility pattern as explained in the present section, we subtract the mean from each series, so that no zero returns remain. Then we remove 2 (3, 0) outliers. This leaves us with 12719 (12621, 12696) observations, respectively. For the bid and ask liquidity curves, no missing values or outliers are present.

The tick size at XETRA depends on the price: For most of our sample period (from January 2009 on), it is €0.001 if the instrument’s price is under €10, €0.005 for prices in the interval [€10, €50), 1 cent for prices from €50 to €100, and 5 cent otherwise. The data set allows us, in principle, to reconstruct LOB_t for any t during a given trading day. Continuous trading on XETRA starts after a 5-minute opening auction at 9am, is interrupted by another auction of this type at 1pm, and ends just before the closing auction at 5:30pm. In our analysis, we take LOB snapshots every 20 minutes, sampled during continuous trading. Specifically, we avoid auction effects by sampling at 9:09am, 9:29am, ..., 12:49pm, and 1:09pm, ..., 5:29pm.

Order book data are typically available only up to a certain “level”, which means that only the volumes at the first 10 or 20 best prices are provided. Therefore, the actual price range covered depends on both the tick size and on how densely the orders are posted. In our case, we have information on *all* admissible price levels. In our analyses, however, we consider only volumes posted at the nearest €2 around the quotes on each market side, a range we expect to suffice to observe all relevant aspects of the LOB. For all three stocks, we record cumulative volumes in increments of one cent, so that the snapshots are of the form

$$\begin{aligned}
 LOB_t := & [P_t^{(bid)}, P_t^{(ask)}, \\
 & v_t^{(bid)}(\text{€}0), v_t^{(bid)}(\text{€}0.01), \dots, v_t^{(bid)}(\text{€}2.00), \\
 & v_t^{(ask)}(\text{€}0), v_t^{(ask)}(\text{€}0.01), \dots, v_t^{(ask)}(\text{€}2.00)]'.
 \end{aligned}$$

Moreover, our data set not only contains the information that was available to the market participants, it also provides a full picture of hidden liquidity as, for example, iceberg orders are included.

2.5.2 Diurnal patterns

The estimated diurnal volatility patterns for the three stocks are shown in the left panel of Figure 3. They basically exhibit the familiar U-shape. In the second half of the day, volatility typically rises after 3:29pm (US markets open at 3:30pm CET) and peaks at 4:09pm, before decreasing somewhat until the end of trading at 5:30pm.

The other panels of Figure 3 show the corresponding liquidity patterns. They are quite similar for the two market sides. Especially at greater distance from the quotes, there is a slight upward trend which may be attributed to the fact that some of these limit orders remain only in the book because they are unlikely to be executed. Still, more than 95 percent of the total limit order volume is cancelled rather than executed. The median lifetime of a limit order is less than one second, and it increases with the distance to the quotes.

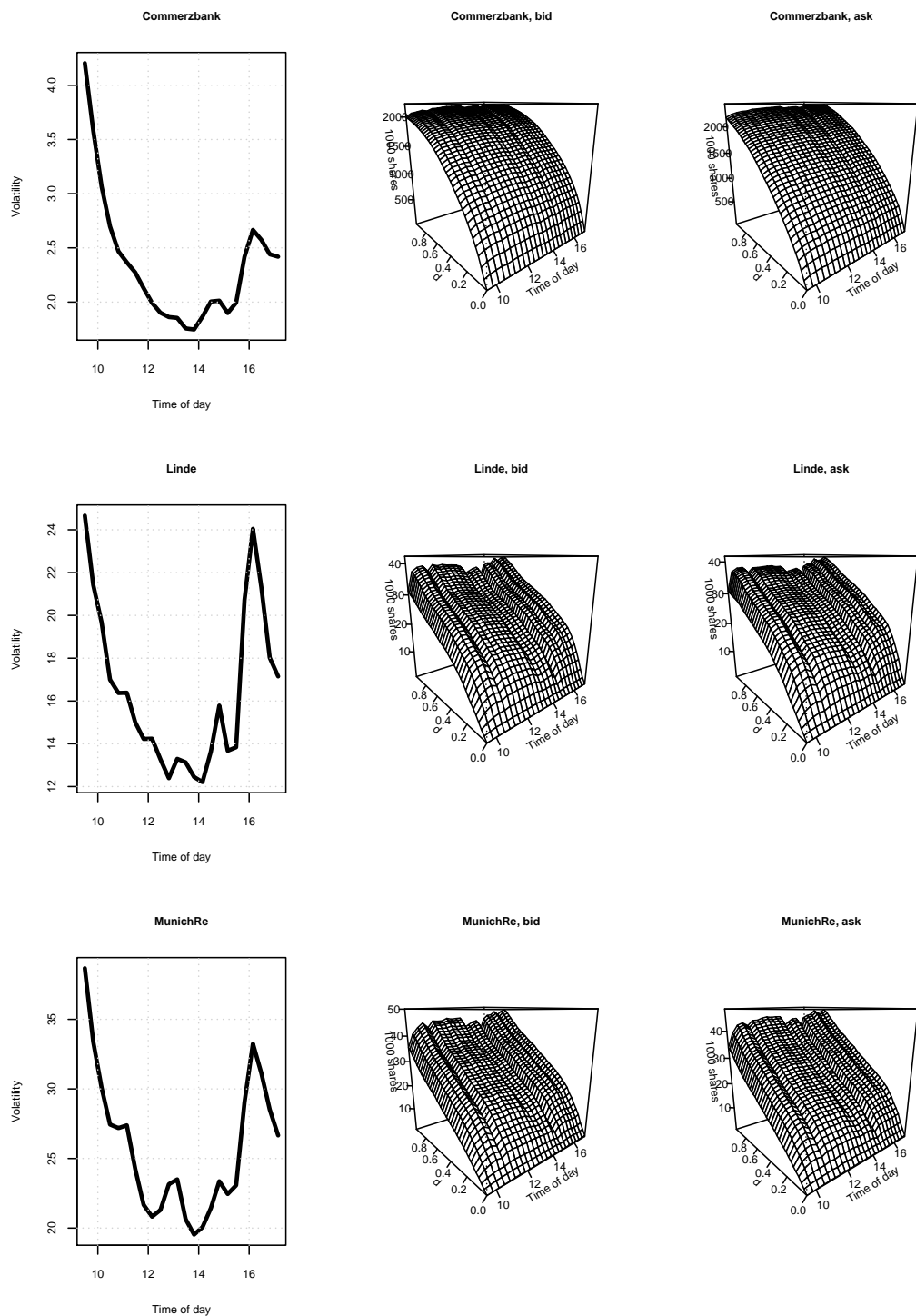


Figure 3: Diurnal volatility (left panel) and liquidity (center and right panel) patterns for the three stocks, fitted using a smoothing spline. From top to bottom: Commerzbank, Linde, and MunichRe.

2.5.3 The structure of liquidity

Next, we analyze the de-seasonalized liquidity over the full sample. The time series of bid and ask-liquidity curves for two exemplary days of the Commerzbank stock are shown in Figure 4. Note that, by construction, the unconditional mean of de-seasonalized liquidity is one for all locations, so that values above (below) one can be interpreted as high (low) liquidity at a specific time of the day and region of the LOB, respectively.

Turning to the functional principal components of the series, the top panel of Figure 5 shows the normalized eigenvalues, i.e., the variances explained by each of the first ten components, for the bid and ask sides, using the whole range of 201 tick levels. For both market sides, four components are needed to capture 95 percent of the variation in liquidity.

In the bottom part of Figure 5, the first four estimated eigenfunctions for both market sides are shown. Note that the eigenfunctions are unique only up to the sign. With this in mind, we conclude that the factor structure of both sides is quite similar. In both cases, the first eigenfunction is almost horizontal and, therefore, can be interpreted as a “level” factor. The remaining eigenfunctions capture different aspects of liquidity variation, all having in common that deviations near the quotes (in the left part of the domain) are larger than at a greater distance from the quotes. This finding reflects the larger variation of liquidity near the quotes, as seen already from Figure 5.

To statistically test for differences in the eigenfunctions, [Benko et al. \(2009\)](#) propose a resampling-based test for equality of eigenfunctions for the two-sample situation encountered here. Instead of applying this test, we estimate the scores, $\xi_{j,t}$, of the truncated FPC expansion, $\hat{x}_t = \sum_{j=1}^4 \xi_{j,t} \hat{\phi}_j$, using OLS regressions of the x_t against the first four eigenfunctions. We find that eigenfunction estimates based only on bid curves, on ask curves, or on both, respectively, yield in all three cases virtually identical score estimates, $\hat{\xi}_{j,t}$, and, hence, approximations $\hat{x}_t = \sum_{j=1}^4 \hat{\xi}_{j,t} \hat{\phi}_j$.

Liquidity, in contrast, is far from symmetric. The contemporaneous correlation of the scores between the two market sides is rather low (see Table 1).

	bid.1	bid.2	bid.3	bid.4
ask.1	-0.27	0.07	-0.04	0.34
ask.2	0.07	-0.02	0.09	-0.15
ask.3	0.08	-0.02	0.03	0.10
ask.4	-0.06	0.34	0.10	-0.08

Table 1: *Contemporaneous sample correlations between the first four FPC score series for the two market sides. Not shown: Correlations between scores of the same market side which are orthonormal by construction.*

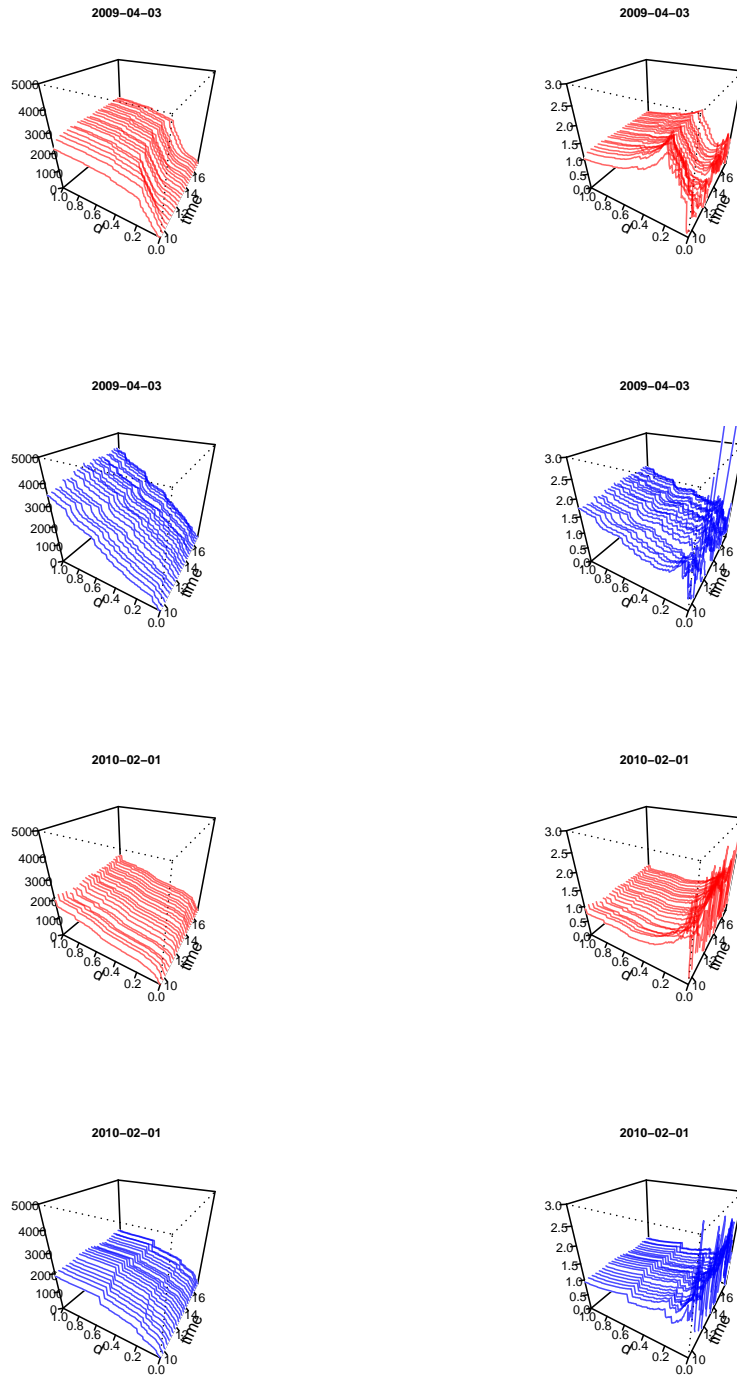


Figure 4: *Functional time series of ask (red) and bid (blue) liquidity curves for April 3, 2009 (top) and February 1, 2010 (bottom), for the Commerzbank stock. The left panel shows the raw data (cumulative number of shares, measured in thousands, within a range of €0 to €2 from the quotes), the right panel shows the de-seasonalized versions of the same curves.*

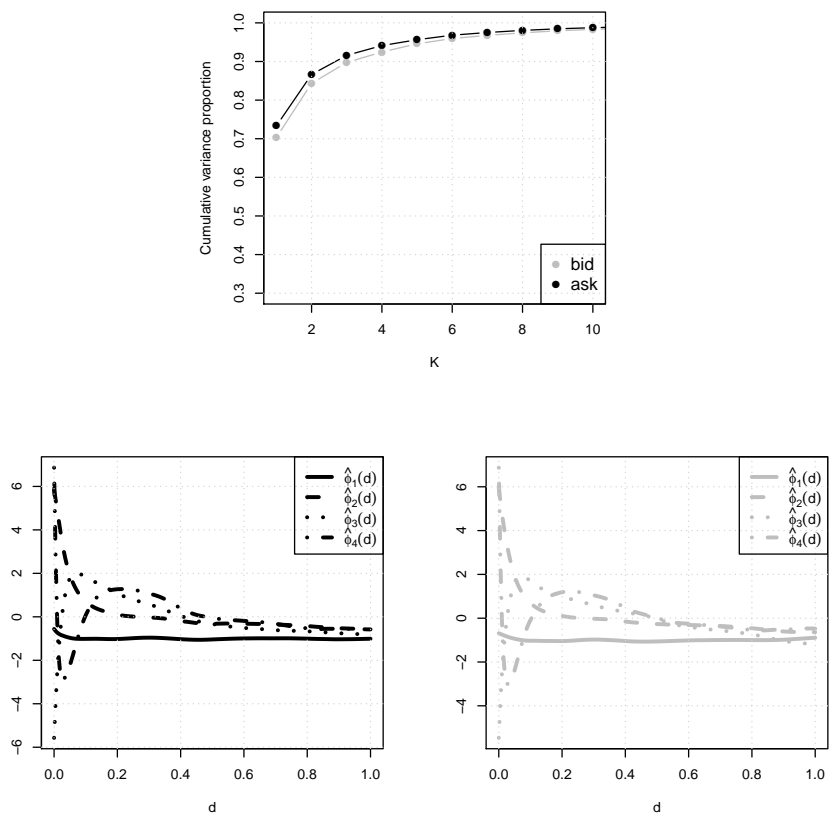


Figure 5: *Top panel: Cumulative normalized eigenvalues of the estimated liquidity covariance operators. Bottom panel: First four estimated eigenfunctions for ask (left) and bid (right) sides, all for Commerzbank. Note that the eigenfunctions are unique only up to the sign.*

3 GARCH-FunXL

3.1 The model

The raw log-returns, $r_{t,i}$, during intraday times $i - 1$ and i on day t , $i = 1, \dots, I$, are assumed to be generated by

$$r_{t,i} = y_{t,i} s_i, \quad (3)$$

$$y_{t,i} = \sigma_{t,i} \varepsilon_{t,i}, \quad \varepsilon_{t,i} \stackrel{iid}{\sim} (0, 1), \quad (4)$$

where s_i is a deterministic diurnal volatility component, and $\sigma_{t,i}$ is the conditional volatility of the de-seasonalized returns, $y_{t,i}$. This setup is as in Andersen and Bollerslev (1997), Andersen and Bollerslev (1998) and Engle and Sokalska (2012), denoted in the following by AB and ES, respectively, with the exception that these authors further decompose σ_t into a daily and an intradaily component. ES use commercially available data based on multifactor risk models for the daily component, whereas AB adopt a GARCH specification. In principle, we could also use these approaches but, at this stage, prefer to keep it simple.

Note that the model generates only intraday returns and assumes that $\sigma_{t,i}$ stays constant between the trading hours of subsequent trading days, i.e., $\sigma_{t,I} = \sigma_{t+1,0}$.

The conditional volatility follows a GARCH specification, which is augmented by exogeneous information in terms of the liquidity curves at the beginning of each intraday interval from both market sides, i.e.,

$$\sigma_{t,i} = f(y_{t,i-1}, \dots, x_{t,i-1}^{(ask)}, x_{t,i-1}^{(bid)}), \quad (5)$$

where $y_{t,i-1}, \dots$ denotes the entire return history, in the following denoted by $\mathcal{F}_{t,i-1}$. As explained in Section 2, the liquidity curves are, as the $y_{t,i}$, de-seasonalized quantities.

In the following, we lighten notation by dropping the i . Furthermore, we consider a log-GARCH specification whose endogeneous parts are of order 1. We let the functional liquidities also enter the model in a log-linear fashion, such that the conditional log-variance becomes

$$\log \sigma_t^2 = \omega + \alpha \log y_{t-1}^2 + \beta \log \sigma_{t-1}^2 \quad (6)$$

$$+ \int_0^1 \gamma^{(ask)}(m) x_{t-1}^{(ask)}(m) dm + \int_0^1 \gamma^{(bid)}(m) x_{t-1}^{(bid)}(m) dm. \quad (7)$$

We denote this larger information set, consisting of past returns plus liquidities at $t - 1$, by \mathcal{F}_{t-1}^L .

Collecting all this and the ingredients from Section 2, the logarithmic GARCH(1,1)-FunXL model for returns with conditional volatility influenced by $x_{t-1}^{(s)}$, $s \in \{\text{bid}, \text{ask}\}$, is defined as follows.

Definition 2 (Logarithmic GARCH(1,1)-FunXL process). *Let $x_t^{(ask)}, x_t^{(bid)}$ be drawn from curve-valued exogeneous liquidity processes as specified above. Then, y_t follows a logarithmic GARCH(1,1)-FunXL process, if*

$$y_t = \sigma_t \varepsilon_t, \quad \varepsilon_t \stackrel{iid}{\sim} (0, 1) \quad (8)$$

$$\begin{aligned} \log \sigma_t^2 &= \omega + \alpha \log y_{t-1}^2 + \beta \log \sigma_{t-1}^2 \\ &+ \int_0^1 \gamma^{(ask)}(m) x_{t-1}^{(ask)}(m) dm + \int_0^1 \gamma^{(bid)}(m) x_{t-1}^{(bid)}(m) dm, \end{aligned} \quad (9)$$

where

$$x_t^{(s)} = \mu^{(s)} + \sum_{k=1}^{\infty} \xi_{k;t}^{(s)} \phi_k^{(s)}. \quad (10)$$

We assume that the terms $\int_0^1 \gamma^{(s)}(m) x_{t-1}^{(s)}(m) dm$, $s \in \{\text{bid}, \text{ask}\}$, are non-degenerate in the sense that the coefficient functions are finite over $[0, 1]$ and recall that both liquidity processes are stationary in the sense explained above, especially having finite mean function and covariance operator. Then, if $|E(\log \varepsilon_t^2)| < \infty$, (8)-(10) admits the ARMA(1,1)-(Fun)X representation

$$\begin{aligned} \log y_t^2 &= \pi_0 + \pi_1 \log y_{t-1}^2 + \theta_1 \log u_{t-1} \\ &+ g\left(x_{t-1}^{(ask)}, x_{t-1}^{(bid)}; \gamma^{(ask)}, \gamma^{(bid)}\right) + u_t, \end{aligned}$$

where

$$\begin{aligned} \pi_0 &= \omega + (1 - \beta)E[\log \varepsilon_t^2], \\ \pi_1 &= \alpha + \beta, \\ \theta_1 &= -\beta, \\ u_t &= \log \varepsilon_t^2 - E[\log \varepsilon_t^2], \\ g\left(x_{t-1}^{(ask)}, x_{t-1}^{(bid)}; \gamma^{(bid)}, \gamma^{(ask)}\right) &= \int_0^1 \gamma^{(ask)}(m) x_{t-1}^{(ask)}(m) dm + \int_0^1 \gamma^{(bid)}(m) x_{t-1}^{(bid)}(m) dm; \end{aligned}$$

see also [Sucarrat et al. \(2013\)](#). An interesting feature is that the intercept and therefore the autocorrelation function of $\log y_t^2$ depends on the innovation distribution via $E[\log \varepsilon_t^2]$. It follows immediately that, for a model of order (1,1), $\log y_t^2$ is stationary if $-1 < \alpha + \beta < 1$.

We choose the log-GARCH specification primarily to avoid non-negativity constraints for the functional exogeneous part of the model: while liquidity *curves*, even if de-seasonalized, are non-negative by construction, the infinite-dimensional liquidity *parameters* are unrestricted over the entire domain. A restriction that guarantees non-negativity of the functional predictors appears hardly to be feasible.

One further attractive feature of log-GARCH specifications is that log volatility has no lower bound (in contrast to the standard GARCH case). A possible drawback could be that the model does not allow for zero returns.²

Another application of the log-GARCH-X, which is in some aspects similar to ours, is the Realized GARCH model of [Hansen et al. \(2012\)](#).

3.2 Estimation

We recall from Section 2 that the liquidity curves can be approximated by their first K functional principal components, i.e.,

$$x_t^{(s)}(d) \approx \mu(d)^{(s)} + \sum_{k=1}^K \phi_k^{(s)}(d) \xi_{k,t}^{(s)}.$$

Assumptions

We make the following assumptions:

- (i) For each s , there is some $K < \infty$ for which

$$\begin{aligned} & \int_0^1 \sum_{j=K+1}^{\infty} \phi_j^{(s)}(m) x_t^{(s)}(m) dm = 0 \\ \Leftrightarrow & \int_0^1 \sum_{j=K+1}^{\infty} \sum_{i=1}^{\infty} \phi_j^{(s)}(m) \phi_i^{(s)}(m) \xi_{i,t}^{(s)} dm = 0 \\ \Leftrightarrow & \int_0^1 \sum_{j=K+1}^{\infty} \sum_{i=K+1}^{\infty} \phi_j^{(s)}(m) \phi_i^{(s)}(m) \xi_{i,t}^{(s)} dm = 0 \end{aligned}$$

holds.

- (ii) This K is the same for both market sides.

This means that only a finite number of liquidity components, and moreover only those that explain liquidity best, have an impact on our quantity of primary interest, the price volatility.

However, this assumption does not rule out dynamic dependencies between the first K and the remaining components. Consider, for example, the following vector autoregressive (VAR) liquidity dynamics for a process whose covariance has $K + L$ non-zero eigenvalues, $L \geq 1$,

²This is, however, not of practical relevance for de-meaned returns. For more details on log-GARCH models see [Francq et al. \(2013\)](#), who use an asymmetric log-GARCH specification (similar to the GJR-GARCH), which could also be adopted here.

$$\boldsymbol{\xi}_t^{(s)} = \begin{bmatrix} \xi_{1,t}^{(s)} \\ \vdots \\ \xi_{K+L,t}^{(s)} \end{bmatrix} = \boldsymbol{\nu}^{(s)} + \sum_{j=1}^p \mathbf{A}_j^{(s)} \boldsymbol{\xi}_{t-j}^{(s)} + \mathbf{v}_t^{(s)},$$

$$x_t^{(s)}(d) = \mu^{(s)}(d) + \sum_{j=1}^{K+L} \phi_j^{(s)}(d) \xi_{j,t}^{(s)},$$

i.e., each liquidity curve can be decomposed into $K + L$ orthonormal components, i.e.,

$$\int_0^1 \phi_i(m) \phi_j(m) dm = 1 \quad \text{for } i = j, \text{ and zero otherwise.}$$

All univariate score processes are contemporaneously uncorrelated with each other, but may well depend on lagged values of other processes. This is ruled out if the autoregressive matrix of the full liquidity process is assumed to be block diagonal in the sense that the first K components' scores do not interact with components $K + 1, \dots, K + L$.

Finally, while not explicitly claiming that the scores have such VAR dynamics, we assume that the lead and lag effects of components $K + 1, \dots$ on the first K components' scores are negligible, which seems to be a reasonable assumption for our data: Fitting VAR models to the empirical FPC scores, we find that autoregressive matrices are nearly diagonal, i.e., each individual score series is mainly driven by its own past.

Two-step estimation

We estimate the GARCH-FunXL model in two steps.

1. Estimation of the liquidity curves, using the orthonormal FPC expansion

$$\hat{x}_t^{(s)}(d) = \hat{\mu}^{(s)}(d) + \sum_{k=1}^K \hat{\phi}_k^{(s)}(d) \hat{\xi}_{k,t}^{(s)},$$

where the true K , mean function μ , and eigenfunctions ϕ_k are unknown, and the $\hat{\xi}_{k,t}^{(s)} = \int_0^1 (x_t^{(s)}(m) - \hat{\mu}^{(s)}(m)) \hat{\phi}_k^{(s)}(m) dm$ are computed via numerical integration. This step has been outlined in detail in Section 2.

2. QML estimation of the GARCH-FunXL parameters, using the scores $\hat{\xi}_{k,t}^{(s)}$, $k = 1, \dots, K$, $t = 1, \dots, T$ from Step 1 and the return data.

For statistical inference conditional on a truncated K -component FPC decomposition of $x_t^{(s)}$, we employ a Gaussian quasi-likelihood approach to obtain estimates of $\omega, \alpha, \beta, \gamma^{(bid)}, \gamma^{(ask)}$. The conditional distribution of the logarithmic GARCH(1,1)-FunXL with Gaussian innovations is given by

$$y_t | \mathcal{F}_{t-1}^L \sim N \left(0, \exp \left(\omega + \alpha \log y_{t-1}^2 + \beta \log \sigma_{t-1}^2 + \int_0^1 \gamma^{(ask)}(m) x_{t-1}^{(ask)}(m) dm + \int_0^1 \gamma^{(bid)}(m) x_{t-1}^{(bid)}(m) dm \right) \right). \quad (11)$$

We do not claim the innovations to be Gaussian, instead we are interested in inference on the latent volatility process only. The Gaussian quasi-log-likelihood is given by

$$l(\mathbf{y}, \mathbf{x}; \omega, \alpha, \beta, \gamma^{(bid)}, \gamma^{(ask)}) = -\frac{1}{2} \sum_{t=2}^T \left(\sigma_t^2 + \frac{y_t^2}{\sigma_t^2} \right),$$

where \mathbf{y} is the vector of de-seasonalized returns, and \mathbf{x} the “matrix” of de-seasonalized liquidity curves.

As both the liquidity curves, $x_t^{(s)}$, and the coefficients, $\gamma^{(s)}(\cdot)$, are infinite-dimensional objects, the term $\int_0^1 \gamma^{(s)}(m) x_t^{(s)}(m) dm$ has to be approximated by some finite-dimensional representation. In our practical application, we use $K = 1, \dots, 5$. For all three stocks considered, $K = 4$ components explain at least 95 percent of the curves’ variation.

Introducing a K -dimensional parameter vector $\boldsymbol{\gamma}^{(s)} = [\gamma_1^{(s)} \quad \dots \quad \gamma_K^{(s)}]$ for each market side, we expand the coefficient function using the same set of K eigenfunctions that is used to represent the curves themselves, i.e.,

$$\gamma^{(s)}(d) = \sum_{k=1}^K \gamma_k^{(s)} \hat{\phi}_k^{(s)}(d),$$

so that, plugging in estimated mean, eigenfunctions and scores from the FPCA of the liquidity curves, the integral $\int_0^1 \gamma^{(s)}(m) x_t^{(s)}(m) dm$ becomes

$$\int_0^1 \sum_{j=1}^K \sum_{k=1}^K \hat{\xi}_{j;t}^{(s)} \hat{\phi}_j^{(s)}(m) \gamma_k^{(s)} \hat{\phi}_k^{(s)}(m) dm = \sum_{k=1}^K \gamma_k^{(s)} \hat{\xi}_{k;t}^{(s)}$$

by orthonormality of the eigenfunctions. This approach is well-known from *functional principal component regression* and its core idea is the same as in PC regression within the usual scalar multiple regression setting. Note that this structural assumption along with the assumption that only a finite number of components affects the conditional variance implies an identification problem: There are infinitely many functions $\phi_j(d)$ which are orthogonal to the K functions appearing in either the “true” or the fitted liquidity representation. Thus, each of these $\phi_j(d)$ could be added to the basis expansion of $\gamma^{(s)}(m)$ without affecting the model’s goodness of fit.

Defining

$$G_{t-1} := \alpha \log y_{t-1}^2 + \beta \log \sigma_{t-1}^2,$$

we can now write the conditional volatility as

$$\begin{aligned}
\log \sigma_t^2 &= \omega + G_{t-1} + \int_0^1 \gamma^{(bid)}(m) x_{t-1}^{(bid)}(m) dm + \int_0^1 \gamma^{(ask)}(m) x_{t-1}^{(ask)}(m) dm \\
&= \omega + G_{t-1} + \sum_s \int_0^1 \gamma^{(s)}(m) x_{t-1}^{(s)}(m) dm \left(\hat{\mu}^{(s)}(m) + \sum_{k=1}^K \hat{\xi}_{t-1;k}^{(s)} \hat{\phi}_k^{(s)}(m) \right) dm \\
&= \omega + G_{t-1} + \underbrace{\sum_s \int_0^1 \gamma^{(s)}(m) \hat{\mu}^{(s)}(m) dm}_{=:\gamma_0^{(s)}} + \sum_{k=1}^K \hat{\xi}_{k;t-1}^{(s)} \underbrace{\int_0^1 \gamma^{(s)}(m) \hat{\phi}_k^{(s)}(m) dm}_{=:\gamma_k^{(s)}} \\
&= \underbrace{\omega'}_{:=\omega+\gamma_0} + G_{t-1} + \sum_s \sum_{k=1}^K \gamma_k^{(s)} \hat{\xi}_{k;t-1}^{(s)}.
\end{aligned} \tag{12}$$

Compared to the original model, the infinite-dimensional problem boils down to estimating $\omega, \alpha, \beta, \gamma_1^{(bid)}, \dots, \gamma_K^{(bid)}, \gamma_1^{(ask)}, \dots, \gamma_K^{(ask)}$, i.e., $2K$ additional scalar parameters. In practice, however, it may pay to be rather generous in choosing K , because the components that explain much of the liquidity variation are not guaranteed to have a large impact on price volatility. Conversely, modes of variation that are rather unimportant for liquidity variation may well be of great importance for predicting price volatility.

Properties of the estimators

Although the inclusion of exogeneous variables (like interest rates or realized volatility) has already been in vogue for some time, theoretical properties of GARCH-X processes and especially QML estimators of their parameters have been established only very recently. Han (2013) and Han and Kristensen (2014) investigate QML estimation for a broad class of possible exogeneous processes, including long-memory and integrated processes, but do so only for linear specifications and univariate exogeneous processes. In particular, in case of a stationary exogeneous process (as assumed here), QMLEs of linear GARCH parameters retain their favorable properties.

According to Sucarrat et al. (2013), Francq et al. (2013), and Hansen et al. (2012), and to the best of our knowledge, such asymptotic results for log-GARCH-X models do not exist. Hansen et al. (2012), based on the results of Straumann et al. (2006), conjecture consistency and asymptotic normality of their QMLE in a scalar log-GARCH-X framework without providing a proof. With our assumptions regarding liquidity effects on volatility, we are basically in a log-GARCH-X setting as well. However, an additional complication is given by the fact that our exogeneous variables, the FPC scores, are generated by a nonparametric procedure in the first place, inducing additional estimation uncertainty. Surprisingly, this fact is rarely addressed in the FDA literature, see for example Yao et al. (2005). This

means that even if the step-two parameter estimates could be shown to be consistent and asymptotically normal, ignoring estimation uncertainty from the first step, i.e., for mean functions, eigenfunctions, and scores, will result in confidence bands for $\gamma^{(s)}(\cdot)$ that are too narrow. An alternative, frequently used in FDA, is to choose a bootstrap approach. For our time series setting, the stationary bootstrap proposed by Politis and Romano (1994), where blocks of random lengths are drawn and reassembled to form resamples of the original series, is most suitable.

Simulation results reported in section 3.4 convey an idea of the properties of QML estimators in our log-linear specification.

3.3 Liquidity impact

The conditional variance of the GARCH-FunXL model can be written as

$$\begin{aligned} \sigma_t^2 = & \exp(\omega + \alpha \log y_{t-1}^2 + \beta \log \sigma_{t-1}^2) \\ & \times \exp\left(\int \gamma^{(ask)}(m)x_{t-1}^{(ask)}(m)dm + \int \gamma^{(bid)}(m)x_{t-1}^{(bid)}(m)dm\right). \end{aligned} \quad (13)$$

that is, as a product of the (endogeneous) GARCH part and the exogeneous liquidity part.

We call the latter, i.e.

$$LI_t := \exp\left(\int \gamma^{(ask)}(m)x_{t-1}^{(ask)}(m)dm + \int \gamma^{(bid)}(m)x_{t-1}^{(bid)}(m)dm\right), \quad (14)$$

the *liquidity impact*. Note that the subindex is chosen according to the target variable, the conditional variance. Due to the multiplicative structure of the model, liquidity reduces volatility for $LI_t < 1$ and increases it for $LI_t > 1$. LI_t can be split up further into the contributions of each market side, $LI_t = LI_t^{(ask)} LI_t^{(bid)}$.

Morover, in analogy to the news impact curve, a three-dimensional plot of LI_t against d and $x_{t-1}^{(s)}(d)$ amounts to a *liquidity impact surface* (LIS). For a given market side, the LIS shows the influence of liquidity on conditional variance at all locations, d , within the LOB. However, as both the functional parameter and the liquidity curves can have quite complex shapes — for instance different signs at different locations of their domain — the interpretation of an LIS is not as straightforward.

The K -truncated, estimated version of the liquidity impact is given by

$$\widehat{LI}_t = \exp\left(\widehat{\gamma}^{(ask)} \widehat{\xi}_{t-1}^{(ask)} + \widehat{\gamma}^{(bid)} \widehat{\xi}_{t-1}^{(bid)}\right).$$

Confidence statements for the liquidity impact are directly linked to estimation uncertainty about the functional parameters discussed above.

3.4 Simulation study

Next, using simulations, we investigate the adequacy of the estimation procedure for our model. In functional regression, the quantity of interest is typically the parameter. In the present study, however, we focus solely on the liquidity impact, which naturally involves the estimation of the functional parameters.

To simulate the process, we specify the liquidity process as in [Aue et al. \(2015\)](#), where the scores follow the VAR process

$$\boldsymbol{\xi}_t^{(s)} = \begin{bmatrix} \xi_{1,t}^{(s)} \\ \vdots \\ \xi_{K,t}^{(s)} \end{bmatrix} = \boldsymbol{\nu}^{(s)} + \sum_{j=1}^p \mathbf{A}_j^{(s)} \boldsymbol{\xi}_{t-j}^{(s)} + \mathbf{v}_t^{(s)},$$

$$x_t^{(s)}(d) = \mu^{(s)}(d) + \sum_{j=1}^K \phi_j^{(s)}(d) \xi_{j,t}^{(s)}.$$

We simulate from a $K = 5$ -dimensional score process with $p = 1$ and $T = 1000, 5000, 10000$. Note that for all data sets under investigation, $K = 4$ components capture more than 95 percent of liquidity variation. We use the eigenfunctions from the FPC representation of the Brownian motion (see [Ash and Gardner \(1975\)](#)),

$$\phi_k(d) = \sqrt{2} \sin(k - 0.5)\pi d,$$

two different sets of eigenvalues, and also two different serial dependence structures for the scores. As eigenvalues, we use (i) the decay as for Brownian motion, $\lambda_k = 4/(2k - 1)^2\pi^2$ and (ii) the empirical decay as estimated from Commerzbank's ask curves. As serial dependence structures we use (i) serial independence, $\mathbf{A}_1 = \mathbf{0}$, and (ii) \mathbf{A}_1 resembling the dependence estimated from Commerzbank's ask curves,

$$\mathbf{A}_1 = \begin{bmatrix} 0.98 & 0.08 & 0.09 & -0.09 & 0.08 \\ 0.01 & 0.82 & -0.37 & 0.03 & -0.09 \\ 0.00 & -0.20 & 0.24 & -0.22 & 0.14 \\ 0.00 & 0.02 & -0.10 & 0.81 & 0.26 \\ 0.00 & -0.01 & 0.04 & 0.11 & 0.76 \end{bmatrix},$$

i.e., with dominant diagonal and low off-diagonal elements.

Empirical versions of $\boldsymbol{\xi}_t^{(s)}$, from which \mathbf{A}_1 can be estimated, are obtained as a by-product of the GARCH-FunXL estimation procedure proposed in Section 3.

The unconditional variance, $\boldsymbol{\Gamma}_\xi(0)$, of a VAR process depends on both the autoregressive matrices, \mathbf{A}_j , and the covariance matrix, $\boldsymbol{\Sigma}_v$, of the innovation vector. As we seek to discriminate between effects due to serial dependence and effects due to score variation, we simulate (i) from processes with identical innovation covariances and different serial dependencies (implying different unconditional covariance matrices), and (ii) from processes with equal unconditional covariance matrices and different serial dependencies (implying different innovation covariance matrices).

We investigate models with only one functional exogeneous process, using three different functional parameter settings: (i) $\gamma(m) = 0.01\phi_1(m)$; (ii) a linear combination of all five eigenfunctions with weights 0.01, 0.004, 0.002, 0.0006, 0.001; and (iii) $\gamma(m) = 0.002(4 + 5m - 10m^2 + 4\cos(5m))$. Thus, parameters for settings (i) and (ii) should be more easily identifiable than for (iii) which is not constructed from eigenfunctions. The implied true liquidity impacts are similar to those found in the data. All function evaluations are on $J = 201$ equidistant grid points in $[0, 1]$.

A summary of the results is shown in Table 2. Not surprisingly, estimation accuracy increases substantially with increasing sample size. Moreover, given the unconditional covariance structure of the scores, identification of the liquidity impact performs comparably well regardless of the functional parameter setting. That is, in terms of liquidity impact it does not matter whether the true functional parameter is a linear combination of liquidity's eigenfunctions or not. Finally, we find that there is no clear connection of the unconditional variance of the scores and the precision of the identification of the liquidity impact.

Note that estimated models which capture the true liquidity impact accurately do not necessarily exhibit functional parameter estimates that are close to their true values. This is due to the identification issue discussed above. It is particularly the case (i) if K , the number of estimated components used in the basis expansion of the parameter, exceeds the true K , and (ii) if the true parameter can not be well approximated in terms of the eigenfunctions ϕ_k of the liquidity process.

If liquidity dynamics are governed by a stable VAR process and T is reasonably large, we find that eigenfunctions can be estimated very accurately. Therefore, in situations where the true functional parameter is a linear combination of these eigenfunctions, its estimation is also accurate. The same holds for confidence bands relying on the conjectured normal asymptotics, despite ignoring the estimation uncertainty about the eigenfunctions.

4 Modeling XETRA returns

We use the GARCH-FunXL specification to model 20-minute snapshots for Commerzbank, MunichRe, and Linde stocks traded on the German XETRA LOB from November 3, 2008 to December 31, 2010.³

We fit logarithmic GARCH-FunXL models of GARCH order (1,1) to the data, considering (i) models with liquidity impact from only one market side (bid or ask); (ii) models with liquidity impact from both market sides; and (iii) models with liquidity imbalance impact only, i.e., with functional regressor $x_t^{(imb)} = x_t^{(ask)} - x_t^{(bid)}$. Moreover, we vary the domain of prices around the quotes taken into account, using $D = 51$ (101, 151, 201), corresponding to the domains $[\text{€}0, \text{€}0.50]$ ($[\text{€}0, \text{€}1.00]$, $[\text{€}0, \text{€}1.50]$, $[\text{€}0, \text{€}2.00]$). By doing this, we assess whether or not it pays to take liquidity far from the quotes into account. Note that D (the width of

³For details on construction of the snapshots and removing deterministic patterns, see Section 2.

the liquidity domain) can be viewed as an additional model parameter.

4.1 Estimation results

The goodness-of-fit is assessed employing the AIC and BIC. Their use in this context is somewhat critical as the number of parameters in the penalty term is $3 + K$ (models with one FunX component) or $3 + 2K$ (two components), ignoring the fact that the FPC scores are constructed regressors, which have been estimated nonparametrically from the liquidity data.

Keeping this in mind, we find that the model with imbalance impact performs worst for all three stocks and all four domains considered. The fit of log-GARCH-FunXL models with imbalance impact is always worse than the fit of the pure log-GARCH model, regardless of the information criterion used. This result indicates that the imbalance measure, by construction, eliminates information on the individual curves which is valuable for predicting the price process. Moreover, the models accounting for both market sides' liquidity outperform those using only one side's liquidity information in virtually all cases.

Table 3 shows the two goodness-of-fit results for these bid+ask models when fitting $K = 0, \dots, 5$ FPCs, where $K = 0$ corresponds to the pure log-GARCH model. We see a considerable improvement of the fit when allowing for liquidity information. In many cases the improvement is largest when introducing the second (not the first!) FPC, whose eigenfunction can induce stronger liquidity impact near the quotes than deeper in the book, see Figure 5. In some cases, even the fifth component improves the fit.

Interestingly, the results are not very sensitive with respect to the choice of D . Note that asymptotically, i.e., for $K \rightarrow \infty$ and $T \rightarrow \infty$ at suitable rates, the liquidity curves are represented perfectly, and the functional parameters converge to their true values. This means that, if liquidity in some parts of the domain $[0, D]$ has no impact, the corresponding functional parameter will converge to zero, and that, asymptotically, models with some given D_i nest models with $D_l < D_i$. Limiting or "tuning" D therefore makes only sense in finite samples. The insensitivity with respect to D that we find empirically indicates that the important aspects of liquidity variation are located in the left part of the domain, i.e., near the quotes. We return to this point when discussing the functional parameter estimates. Moreover, the insensitivity may imply that models with large D capture those near-the-quotes aspects of liquidity similarly well as models with smaller D .

Figure 6 depicts the functional parameter estimates for the three stocks considered and the models with both bid and ask liquidity impact. Using the conjecture that the QML estimator of $\boldsymbol{\theta} = (\omega, \alpha, \beta, \boldsymbol{\gamma}^{(bid)}, \boldsymbol{\gamma}^{(ask)})$, where $\boldsymbol{\gamma}^{(s)} = (\gamma_1^{(s)} \cdots \gamma_K^{(s)})'$, is asymptotically normal (see Section 3.2), and assuming the estimation error for the eigenfunctions to be negligible, confidence bands are constructed as follows. We denote the the covariance matrix of $\boldsymbol{\theta}$ by $\boldsymbol{\Sigma}_{\boldsymbol{\theta}}$. $\boldsymbol{\Sigma}_{\boldsymbol{\theta}}$ contains $K \times K$ -dimensional partitions, $\boldsymbol{\Sigma}_{\boldsymbol{\gamma}^{(s)}}$, given by the covariance matrices of $\boldsymbol{\gamma}^{(s)}$. We stack the corresponding eigenfunctions, $\phi_k^{(s)}$, $k = 1, \dots, K$, in the "vector"

$$\Phi^{(s)} = [\phi_1^{(s)} \quad \dots \quad \phi_K^{(s)}]'$$

The covariance kernel of the functional parameter $\gamma^{(s)}(m)$ is then given by

$$\Sigma_{\gamma^{(s)}}(d, m) = \Phi'^{(s)}(d) \Sigma_{\gamma}^{(s)} \Phi^{(s)}(m).$$

Plugging in estimates of $\Phi^{(s)}$ and $\Sigma_{\gamma^{(s)}}$, standard errors of $\hat{\gamma}^{(s)}$ are given by the square root of the kernel estimate's diagonal, $\left(\hat{\Sigma}_{\hat{\gamma}^{(s)}}(d, d)\right)^{1/2}$.

All estimates have in common that both the effect and its uncertainty are largest at the left boundary of the domain, i.e., near the quotes. High bid liquidity near the quotes tends to increase, high ask liquidity tends to decrease volatility (with the exception of Commerzbank). The local impact tends to vanish for liquidity deeper in the book. However, none of the estimates is strictly positive or negative over the entire domain of relative prices. Moreover, the sizes of the local liquidity effects on the conditional variance are hard to interpret and compare anyway, particularly between different stocks. As a consequence, we advocate the interpretation of the cumulative impact, LI_t , instead.

4.2 Liquidity impact

Liquidity impact is the cumulative effect of liquidity on the conditional variance over the entire domain of relative prices. Figure 7 depicts the estimated liquidity impact trajectories implied by the models with functional parameter estimates shown in Figure 6. Note that liquidity impact appears to be fairly robust with respect to the specific choice of K . The results for $K = 2, 4, 5$ are quite similar. Also, we find the impact not only to be time-varying, but to differ in size and direction, both between stocks and between market sides for the same stock. For instance, for Commerzbank, the liquidity contribution to volatility is typically large as compared to Linde. The unconditional distribution of LI_t for Commerzbank is heavily skewed to the right (with many volatility-increasing outbursts), whereas it is fairly symmetric or even slightly left-skewed for Linde and MunichRe.

As LI_t is a linear combination of the FPC scores of the liquidity processes, it inherits its autocorrelation structure from $\xi_t^{(s)}$. As most elements of $\xi_t^{(s)}$ are highly persistent, so is LI_t , as is shown in Figure 8.

4.3 Forecasting

Is liquidity information helpful in improving the forecasting performance? To answer this question, we conduct an out-of-sample forecast exercise. We follow [Engle and Sokalska \(2012\)](#) and use the negative quasi-log-likelihood (QLIKE) of one-step-ahead volatility forecasts as loss function. An alternative method of forecast evaluation would be the use of realized measures of volatility. However, such measures are expected to be very noisy in a high-frequency setting, even if subsampling or other measures, supposedly alleviating the impact of microstructure noise, are used in RV estimation.

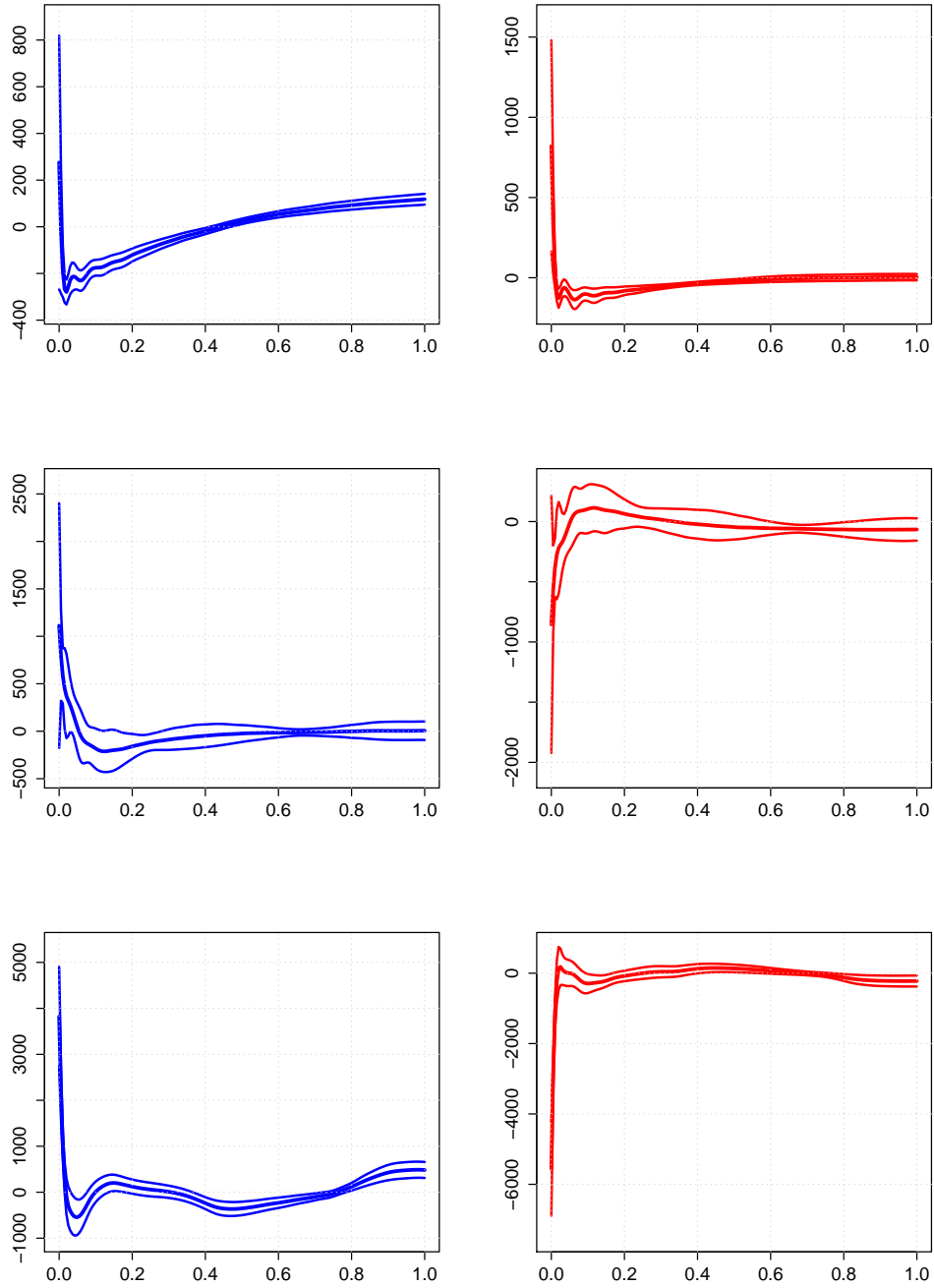


Figure 6: *Estimated functional parameters for Commerzbank (top panel), MunichRe (center panel), and Linde (bottom panel), along with 95 percent confidence bands. Results are for models with both bid (left) and ask (right) liquidity impact, with $K = 3$ liquidity components, and $D = 201$ relative price levels. The confidence bands are based on the conjectured asymptotic normality. Estimation uncertainty from step 1 (eigenfunctions) is assumed to be negligible.*

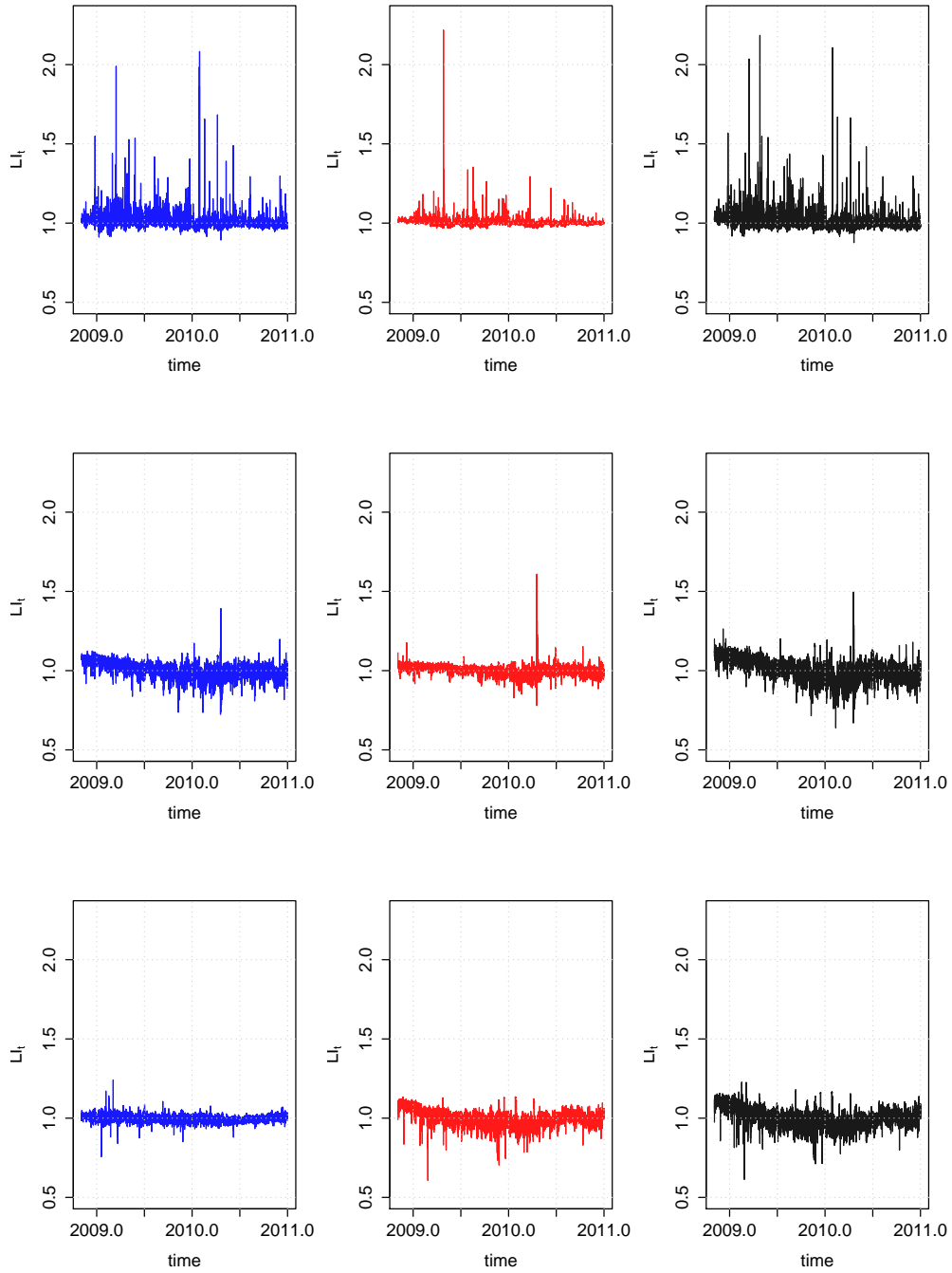


Figure 7: *Estimated liquidity impact for the models with two functional liquidity processes, $K = 3$, $D = 201$. From left to right: Bid impact (blue), ask impact (red), and cumulative impact (their product, black). From top to bottom: Commerzbank, MunichRe, and Linde.*

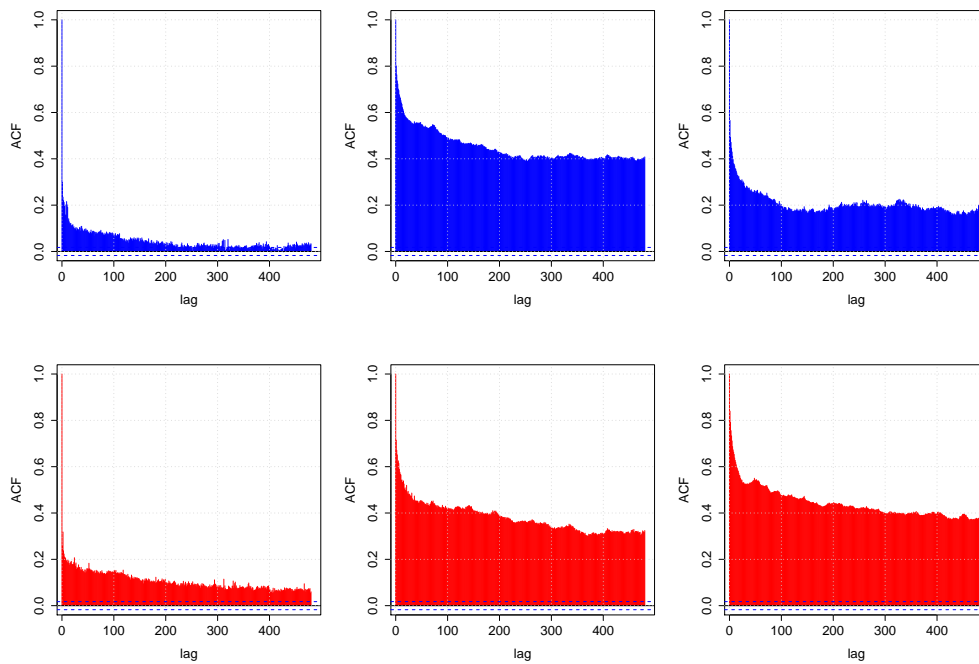


Figure 8: *Sample autocorrelation functions of the estimated liquidity impact for the models with two functional liquidity processes, $K = 3$, and $D = 201$, for the first 480 lags (roughly four weeks). Both bid (top, blue) and ask (bottom, red) impacts are highly persistent for all stocks — Commerzbank (left), MunichRe (center), Linde (right) —, and market sides.*

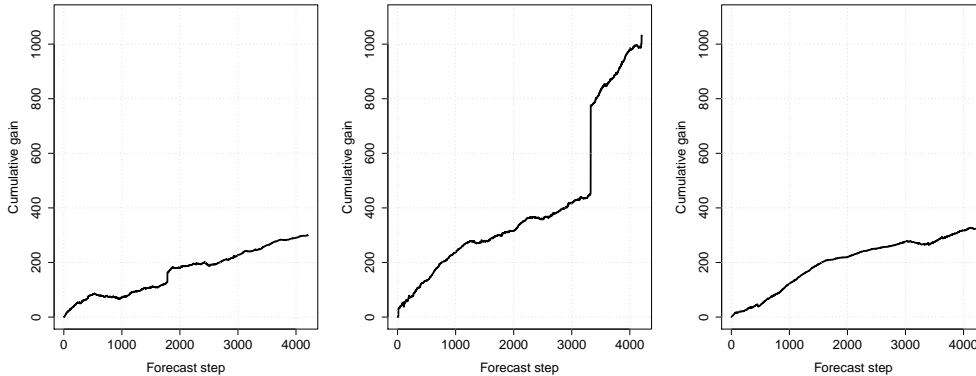


Figure 9: *Cumulative gains in out-of-sample predictive power, i.e., $QLIKE(\text{pure log-GARCH}) - QLIKE(\text{log-GARCH-FunXL})$, from liquidity-driven GARCH models ($K = 3, D = 51$), as compared to models without liquidity impact, for Commerzbank (left), MunichRe (center), and Linde (right).*

Starting with the first two thirds of the available observations, $1 : \lfloor \frac{2}{3}T \rfloor$, we reestimate all models considered above for each forecast step (i.e., $T - \lfloor \frac{2}{3}T \rfloor - 1$ times) in an expanding window scheme. The sum over all one-step-ahead negative log-likelihoods is shown in Table 4.

As before, the models accounting for both market sides yield the best results. For all stocks considered, most of the GARCH-FunXL models provide highly significant QLIKE improvements. Given that forecasting exercises tend to favor parsimonious models, it is noteworthy that in all cases models with $K = 4$, i.e., with as many as eleven parameters deliver the best forecasts. There is also strong evidence that models with $D = 51$ or $D = 101$ outperform their competitors, indicating that liquidity deep in the book is of limited relevance to volatility prediction. Interestingly, this finding is much more pronounced for Linde than for Commerzbank, although throughout the sample Commerzbank's price is much lower than that of Linde, so that a price change by D cents implies a much higher relative change for Commerzbank than for Linde.

Figure 9 depicts the step-by-step cumulative difference in QLIKE between log-GARCH-FunXL and pure log-GARCH, for models with $D = 51$ and $K = 3$. It shows that GARCH-FunXL improves over the pure GARCH specification at a constant rate. Moreover, some large jumps indicate that also extreme returns can be better predicted by using liquidity information.

5 Conclusion

In the present paper, we have put forward a class of semiparametric GARCH-X models with functional exogeneous variables. The model is able to capture the impact of liquidity, as implied by a limit order book, on asset price volatility. In our simulations and applications to stock data, we have confined ourselves to a log-GARCH version of the model which conveniently allows for the inclusion

of complex, potentially negative functional predictors. In many aspects, linear GARCH models are better understood and more tractable than log-linear versions like log-GARCH or EGARCH. Therefore, an alternative GARCH-FunXL specification could, for example, use the framework of [Amado and Teräsvirta \(2013\)](#), i.e., a product of a linear endogeneous GARCH part and a suitable transformation of the exogeneous functional variables.

In an application to the German XETRA limit order book, we have shown that the GARCH-FunXL model can successfully predict intraday volatility. While originally tailored for limit order book data, the model may be useful in other fields of application as well. For example, the term structure of interest rates can be viewed as a functional time series. A further extension that we address in future research is financial duration modeling with functional exogeneous liquidity. The duration analogue to the log-GARCH-FunXL in this paper is an extension of the log-ACD of [Bauwens and Giot \(2000\)](#).

$\gamma(m)$	$T = 1000$						$T = 5000$						$T = 10000$					
	ind.		dep.		ind.		dep.		ind.		dep.		ind.		dep.			
	(a)	(b)	(b)	(c)														
(i)	0.0095 (0.0061)	0.0103 (0.0073)	0.0042 (0.0032)	0.0232 (0.0302)	0.0016 (0.0011)	0.0018 (0.0011)	0.0008 (0.0006)	0.0040 (0.0040)	0.0008 (0.0005)	0.0009 (0.0005)	0.0003 (0.0002)	0.0022 (0.0028)	0.0095 (0.0005)	0.0009 (0.0005)	0.0003 (0.0002)	0.0022 (0.0028)		
(ii)	0.0092 (0.0057)	0.0096 (0.0058)	0.0039 (0.0032)	0.0151 (0.0113)	0.0016 (0.0011)	0.0019 (0.0012)	0.0006 (0.0004)	0.0039 (0.0046)	0.0010 (0.0006)	0.0008 (0.0005)	0.0004 (0.0003)	0.0018 (0.0023)	0.0010 (0.0006)	0.0008 (0.0005)	0.0004 (0.0003)	0.0018 (0.0023)		
(iii)	0.0097 (0.0072)	0.0108 (0.0067)	0.0036 (0.0028)	0.0057 (0.0040)	0.0018 (0.0010)	0.0020 (0.0012)	0.0006 (0.0005)	0.0010 (0.0006)	0.0009 (0.0005)	0.0008 (0.0006)	0.0003 (0.0003)	0.0004 (0.0003)	0.0009 (0.0005)	0.0008 (0.0006)	0.0003 (0.0003)	0.0004 (0.0003)		

Table 2: Mean (standard deviation) of the MSE of liquidity impact computed over $B = 100$ simulation runs, for functional parameters (i)-(iii), serially independent (ind.) vs. dependent (dep.) score processes, and unconditional covariance matrices (a) to (c) (with increasing diagonal elements). Innovation covariance matrices are diagonal with elements decaying from top left to bottom right. In case of serial independence, the eigenstructure is the empirical one (Commerzbank ask curves) up to a constant. Dependence is VAR(1) with autoregressive matrix estimated from Commerzbank ask curves' FPC scores.

Commerzbank								
K	AIC				BIC			
	51	101	151	201	51	101	151	201
0	42995	42995	42995	42995	43017	43017	43017	43017
1	42977	42980	42982	42974	43014	43017	43020	43012
2	42650	42807	42874	42837	42702	42859	42926	42889
3	42631	42638	42643	42598	42698	42705	42710	42665
4	42608	42611	42638	42598	42690	42693	42719	42680
5	42551	42603	42612	42509	42648	42699	42709	42606
MunichRe								
K	AIC				BIC			
	51	101	151	201	51	101	151	201
0	41787	41787	41787	41787	41809	41809	41809	41809
1	41612	41466	41410	41366	41650	41504	41447	41404
2	41119	41039	41061	41057	41171	41091	41113	41109
3	41105	41039	41050	41035	41172	41106	41117	41102
4	41069	41033	41042	41028	41151	41115	41124	41110
5	41062	41034	41031	41029	41159	41130	41128	41125
Linde								
K	AIC				BIC			
	51	101	151	201	51	101	151	201
0	43517	43517	43517	43517	43539	43539	43539	43539
1	43236	43205	43200	43205	43273	43242	43238	43242
2	43212	43206	43204	43208	43264	43258	43256	43260
3	43210	43202	43196	43188	43277	43269	43263	43255
4	43189	43187	43185	43184	43271	43269	43267	43266
5	43192	43188	43181	43184	43289	43285	43278	43281

Table 3: *Goodness-of-fit measures of the models with bid and ask liquidity impact for the three stocks. The number of price levels apart from the quotes considered when constructing the liquidity curves is $D = 51$ (101, 151, 201), corresponding to the domains $[\text{€}0, \text{€}0.50]$ ($[\text{€}0, \text{€}1.00]$, $[\text{€}0, \text{€}1.50]$, $[\text{€}0, \text{€}2.00]$).*

K	Commerzbank				MunichRe				Linde			
	51	101	151	201	51	101	151	201	51	101	151	201
0	2912	2912	2912	2912	4066	4066	4066	4066	4700	4700	4700	4700
1	2977	2785	2858	2860	3822	3767	3613	3554	4425	4345	4840	4884
2	2586	2764	2759	2758	3019	3284	3165	3091	4381	4337	4822	4856
3	2608	2515	2567	2573	3035	3290	3103	3020	4377	4328	4824	4856
4	2613	2602	2619	2577	2993	3248	3142	3067	4293	4303	4807	4848
5	2619	2608	2663	2782	3034	3242	3193	3068	4302	4266	4796	4838

Table 4: *Negative out-of-sample likelihoods for one-step-ahead forecasts of GARCH-FunXL models with bid and ask liquidity impacts. The number of price levels apart from the quotes considered when constructing the liquidity curves is $D = 51$ (101, 151, 201), corresponding to the domains $[\text{€}0, \text{€}0.50]$ ($[\text{€}0, \text{€}1.00]$, $[\text{€}0, \text{€}1.50]$, $[\text{€}0, \text{€}2.00]$).*

References

- Amado, C. and T. Teräsvirta (2013). Modelling volatility by variance decomposition. *Journal of Econometrics* 175(2), 142–153.
- Andersen, T. G. and T. Bollerslev (1997). Intraday periodicity and volatility persistence in financial markets. *Journal of Empirical Finance* 4(2), 115–158.
- Andersen, T. G. and T. Bollerslev (1998). Deutsche mark–dollar volatility: intraday activity patterns, macroeconomic announcements, and longer run dependencies. *The Journal of Finance* 53(1), 219–265.
- Ash, R. B. and M. F. Gardner (1975). *Topics in Stochastic Processes*. New York: Academic Press.
- Aue, A., D. D. Norinho, and S. Hörmann (2015). On the prediction of stationary functional time series. *Journal of the American Statistical Association* 110(509), 378–392.
- Bauwens, L. and P. Giot (2000). The logarithmic acd model: An application to the bid-ask quote process of three nyse stocks. *Annales d’Economie et de Statistique* (60), 117–149.
- Benko, M., W. Härdle, and A. Kneip (2009). Common functional principal components. *The Annals of Statistics* 37(1), 1–34.
- Bowsher, C. G. (2004). Modelling the dynamics of cross-sectional price functions: an econometric analysis of the bid and ask curves of an automated exchange. *Working Paper, Nuffield College, University of Oxford*.
- Bowsher, C. G. and R. Meeks (2008). The dynamics of economic functions: Modeling and forecasting the yield curve. *Journal of the American Statistical Association* 103(484), 1413–1437.
- Cardot, H., F. Ferraty, and P. Sarda (1999). Functional linear model. *Statistics & Probability Letters* 45(1), 11–22.
- Di, C.-Z., C. M. Crainiceanu, B. S. Caffo, and N. M. Punjabi (2009). Multilevel functional principal component analysis. *The Annals of Applied Statistics* 3(1), 458.
- Engle, R. (2000). The econometrics of ultra-high-frequency data. *Econometrica* 68(1), 1–22.
- Engle, R. F. and J. R. Russell (1998). Autoregressive conditional duration: A new model for irregularly spaced transaction data. *Econometrica* 66(5), 1127–1162.
- Engle, R. F. and M. E. Sokalska (2012). Forecasting intraday volatility in the us equity market. multiplicative component garch. *Journal of Financial Econometrics* 10(1), 54–83.
- Francq, C., O. Wintenberger, and J.-M. Zakoïan (2013). Garch models without positivity constraints: Exponential or log garch? *Journal of Econometrics* 177(1), 34–46.
- Gallant, A. R. (1981). On the bias in flexible functional forms and an essentially unbiased form: the fourier flexible form. *Journal of Econometrics* 15(2), 211–245.
- Gallant, A. R., P. E. Rossi, and G. Tauchen (1992). Stock prices and volume. *Review of Financial Studies* 5(2), 199–242.
- Gouriéroux, C., G. Le Fol, and B. Meyer (1998). Étude du carnet d’ordres. *Banque et Marchés* 36, 5–20.

- Han, H. (2013). Asymptotic properties of garch-x processes. *Journal of Financial Econometrics* (forthcoming).
- Han, H. and D. Kristensen (2014). Asymptotic theory for the qmle in garch-x models with stationary and non-stationary covariates. *Journal of Business & Economic Statistics* (forthcoming).
- Hansen, P. R., Z. Huang, and H. H. Shek (2012). Realized garch: a joint model for returns and realized measures of volatility. *Journal of Applied Econometrics* 27(6), 877–906.
- Härdle, W. K., N. Hautsch, and A. Mihoci (2012). Modelling and forecasting liquidity supply using semiparametric factor dynamics. *Journal of Empirical Finance* 19(4), 610–625.
- Hörmann, S. and P. Kokoszka (2010). Weakly dependent functional data. *The Annals of Statistics* 38(3), 1845–1884.
- Hyndman, R. J. and H. L. Shang (2009). Forecasting functional time series. *Journal of the Korean Statistical Society* 38(3), 199–211.
- Jones, C., G. Kaul, and M. Lipson (1994). Transactions, volume, and volatility. *Review of Financial Studies* 7(4), 631–651.
- Patton, A. J. (2011). Volatility forecast comparison using imperfect volatility proxies. *Journal of Econometrics* 160(1), 246–256.
- Politis, D. N. and J. P. Romano (1994). The stationary bootstrap. *Journal of the American Statistical Association* 89(428), 1303–1313.
- Staniswalis, J. G. and J. J. Lee (1998). Nonparametric regression analysis of longitudinal data. *Journal of the American Statistical Association* 93(444), 1403–1418.
- Straumann, D., T. Mikosch, et al. (2006). Quasi-maximum-likelihood estimation in conditionally heteroscedastic time series: a stochastic recurrence equations approach. *The Annals of Statistics* 34(5), 2449–2495.
- Sucarrat, G., S. Grønneberg, and A. Escribano (2013). Estimation and inference in univariate and multivariate log-garch-x models when the conditional density is unknown. *Working Paper*.
- Xiao, L., Y. Li, and D. Ruppert (2013). Fast bivariate p-splines: the sandwich smoother. *Journal of the Royal Statistical Society: Series B (Statistical Methodology)* 75(3), 577–599.
- Yao, F., H.-G. Müller, and J.-L. Wang (2005). Functional linear regression analysis for longitudinal data. *The Annals of Statistics* 33(6), 2873–2903.